Theor Chem Acc (2012) 131:1243
DOI 10.1007/s00214-012-1243-6

REGULAR ARTICLE

Quantum chemical study of self-doping PPV oligomers: spin distribution of the radical forms

D. Geldof · A. Krishtal · F. Blockhuys · C. Van Alsenoy

Received: 29 February 2012 / Accepted: 22 May 2012 / Published online: 14 June 2012

Abstract A quantum chemical study was performed on ten different self-doping PPV oligomers. The geometry and the different weak intramolecular interactions were studied. The atomic spin populations were calculated using the FOHI method and related to the calculated EPR parameters. The effects of the removal of methoxy groups, the introduction of nitrogen atoms, and the relocation of the self-doping sidechain on the geometry, the spin distribution, and the EPR parameters have been described.

Keywords FOHI partitioning method · Self-doping PPV oligomers · Spin density · EPR parameters

1 Introduction

Within the class of oligomeric or low-molecular-weight organic semiconductors distyrylbenzenes (DSBs)—oligomers of poly(*p*-phenylene vinylene) or PPV and their derivatives enjoy a great deal of interest as new materials for opto-electronic applications such as organic light-emitting diodes (OLEDs) [1–7], gas- and ion-selective sensors [8, 9, 10, 11], organic memories, and nonlinear optics (NLO) [12]. In a number of these applications, the oligomers need to be in their electrically conducting state (the neutral compounds are electrical insulators) and this can be easily achieved by oxidizing or reducing them using either a chemical or an electrochemical procedure; the latter has the advantage that the active material can be electro-deposited from a standard electrochemical cell directly onto a pre-chosen substrate. In order to increase the purity of the deposited material, the necessary background electrolyte can be eliminated from the cell by covalently binding it to the oligomer backbone, giving rise to self-doping oligomers (Fig. 1) [13].

As useful and interesting as these new materials may be, further studies of the properties of this new type of oligomer—in particular, the spin (de)localization in their electrically conducting radical form—are hampered somewhat by the fact that self-doping oligomers in their native, undoped form are difficult to prepare and even more difficult to purify: the simultaneous presence of the polar, ionic, self-doping side chain, and the bulky apolar backbone of the oligomer results in the compounds being equally soluble in both polar (even water) and apolar solvents, and conventional ways of purification such as extraction and recrystallization are useless. Since the ionic side chain is present from the very start of the multi-step synthetic pathway [13], purification of the intermediates is skipped, leading to an accumulation of impurities in the final self-doping oligomer and, in general, a decrease in the yields of the various reactions. Introduction of the self-doping chain at the end is impractical, as the Wittig reaction—traditionally used to prepare DSBs—is incompatible with the free hydroxyl group that would necessarily be present on the oligomer during the entire synthetic

Published as part of the special collection of articles celebrating theoretical and computational chemistry in Belgium.

Electronic supplementary material The online version of this article (doi:10.1007/s00214-012-1243-6) contains supplementary material, which is available to authorized users.

D. Geldof · A. Krishtal · F. Blockhuys · C. Van Alsenoy (✉)
Department of Chemistry, University of Antwerp, Universiteitsplein 1, 2610 Antwerp, Belgium
e-mail: kris.vanalsenoy@ua.ac.be

A. Krishtal
Fachbereich Chemie, Technische Universität Kaiserslautern, Erwin Schrödinger Straße, 67663 Kaiserslautern, Germany

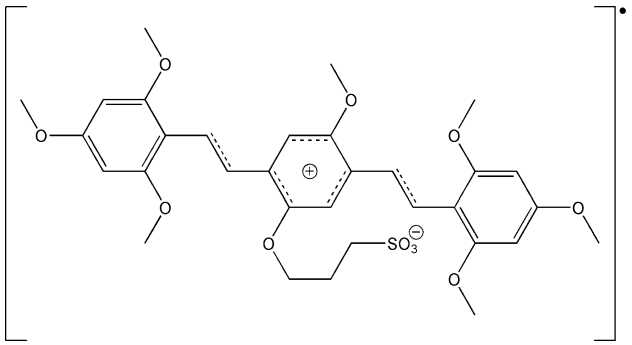

Fig. 1 Schematic representation of the self-doped radical form of *E, E*-2-(3-sulfopropoxy)-5-methoxy-1,4-bis[2-(2,4,6-trimethoxyphenyl) ethenyl]benzene

pathway. The use of protecting groups for this hydroxyl group would make an already lengthy preparative procedure even longer.

Other synthetic procedures, however, do not display this incompatibility with free hydroxyl groups and would allow the preparation and purification of an OH-substituted oligomer, which could then, in the final step, be equipped with a self-doping side chain. The benzylidene-aniline (BA) condensation, used to prepare DSBs in which the spacers are CH=N rather than CH=CH [14, 15], is one such procedure and oligomers such as 5 and 6 (Fig. 2) would become available. Naturally, the introduction of nitrogen atoms in the carbon backbone of the oligomers leads to a rearrangement of the electron density, not only of the native, undoped material but also of the self-doped system, which would result in properties that differ considerably from those of, for instance, the original all-carbon material (1) [13, 16].

The most efficient way to gauge the effects of changes in the molecular structure in terms of the electron distribution is by performing quantum chemical calculations at a suitably reliable level, rather than preparing the compounds and determining their properties experimentally. In this paper, the results of a quantum chemical study on the structure and electronic properties of a series of derivatives of *E, E*-2-(3-sulfopropoxy)-5-methoxy-1,4-bis[2-(2,4,6-trimethoxyphenyl)ethenyl]benzene (1) (Fig. 2) are presented. Apart from the geometries of the non-oxidized, native systems, and those of the self-doped forms in different conformations, the main focus of the paper is on the charge and spin distribution of the self-doped radicals and the influence of the presence and/or position of heteratoms and substituents thereon; compound 1 will be used as a reference structure. Replacement of the ether-oxygen atom of the self-doping chain by nitrogen $(1 \rightarrow 3)$ as well as the removal of the methoxy group on the central ring $(1 \rightarrow 2$ and $3 \rightarrow 4)$ will be investigated. Introduction of nitrogen atoms in the vinyl spacer *alpha* to the central $(1 \rightarrow 5)$ and *alpha* to the peripheral rings $(1 \rightarrow 6)$ leads to the two BA derivatives. Finally, the self-doping side chain will be moved to one of the peripheral rings (7) and the two methoxy groups on the central one are removed (9). The introduction of one (8) or two nitrogen atoms (10) into the latter structure will also be studied. The paper will be concluded with a short discussion of the hyperfine coupling constants calculated for the different derivatives, in the context of those experimentally determined for the reference structure (1).

2 The FOHI method

In this work, we use the fractional occupation Hirshfeld-I (FOHI) method, which is an extension of the Hirshfeld-I (HI) method to calculate atomic spin populations. In the original Hirshfeld method [17], a weight function is used to partition the molecular density $\rho(\vec{r})$ into atomic densities $\rho_a(\vec{r})$:

$$\rho_a(\vec{r}) = w_a(\vec{r})\rho(\vec{r}). \tag{1}$$

The method is based on the use of diffuse boundaries in which the weight function of an atom a can be in principle nonzero in every point $\vec{r}$ of space. The "share" of each atom at point $\vec{r}$ is calculated using:

$$w_a(\vec{r}) = \frac{\rho_a^{[0]}(\vec{r})}{\sum_b \rho_b^{[0]}(\vec{r})} \tag{2}$$

The promolecular density, the denominator in Eq. (2), is defined as the sum of the densities of the isolated atoms $\rho_b^{[0]}$, positioned at the same coordinates as the atomic nuclei in the real molecule. Integration of the atomic density leads to the population of every atom:

$$N_a = \int \rho_a(\vec{r})\mathrm{d}\vec{r} = \int w_a(\vec{r})\rho(\vec{r})\mathrm{d}\vec{r}. \tag{3}$$

This procedure suffered from a number of shortcomings, the most prominent of them being the arbitrary choice of the free atom densities used to construct the promolecular density [18, 19]. Although some of these were corrected in an iterative version of the procedure (the HI method), change in spin, of importance in open shell systems, was not taken into account. This point was remedied in the fractional occupation Hirshfeld-I method (FOHI) through the use of separate weight functions for α and β spin densities. The weight function for the α electrons is given by

$$w_A^{\alpha}(\vec{r}) = \frac{\rho_A^{\alpha}(\vec{r})}{\sum_B \rho_B^{\alpha}(\vec{r})} \tag{4}$$

Equivalent formulas are used for the β density. The spherical symmetry of the free atom densities was ensured

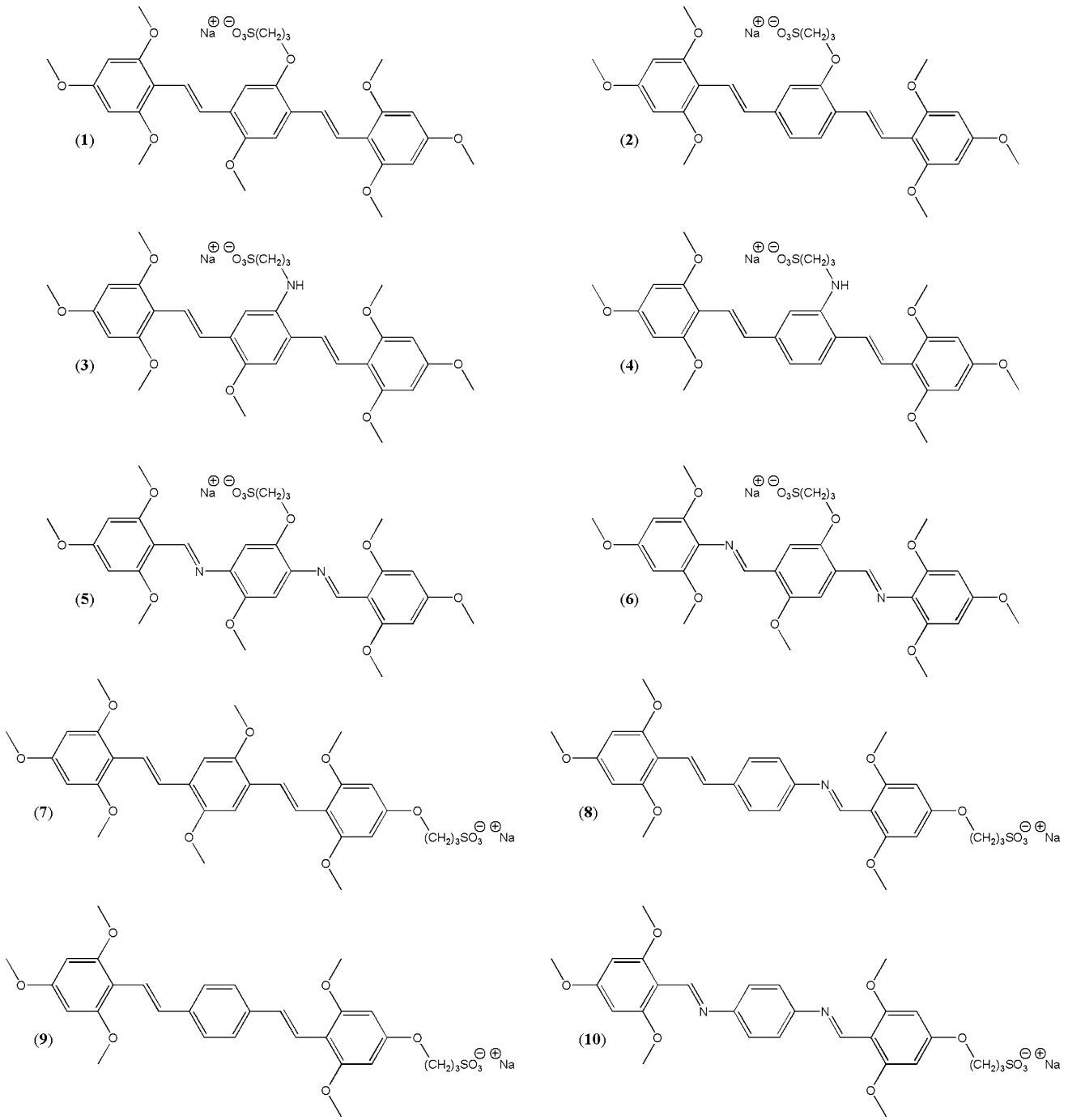

Fig. 2 Structural formulas of the native materials under investigation

through the use of fractional occupations for degenerate atomic orbitals. We refer to the original paper for further details [20].

3 Computational details

For the oligomers depicted in Fig. 2, the geometries were optimized for the neutral, anionic, and radical forms using the B3LYP functional [21–24] and the 6-311+G* basis set [25] with the Gaussian09 program [26]. The EPR parameters were calculated with the ORCA package [27] using the B3LYP functional combined with the EPR-II basis set [28] for the carbon, hydrogen, and nitrogen atoms and the Ahlrichs-SVP basis set [29, 30] for the oxygen and sulfur atoms. Identical basis sets were chosen as used in previous calculations [16]. For the fractional occupation Hirshfeld-I partitioning (FOHI), the atomic densities were calculated at

every iteration using the BRABO program [31] with the B3LYP functional and 6-311+G* basis set. The FOHI charge and spin populations were evaluated by making use of the STOCK program [32]. Both programs are part of the BRABO package. The geometries of the neutral and anionic forms can be found in the supplementary material.

4 Results and discussion

4.1 Geometry and atomic charges

For each of the ten oligomers, a number of geometry optimizations were performed: (1) the neutral structure (presented in Fig. 2), (2) the "anionic" structure which is obtained by removing the sodium atom from the neutral structure, and (3) the two conformations of the radical form given in Fig. 3. In the following, only the radical structures will be discussed.

Two different structures can be envisaged for the self-doped systems, that is, the radical form of the oligomers: (1) a structure in which the sulfonated alkyl chain is extended from the conjugated backbone of the oligomer (Fig. 3a), which will be designated "extended structure," and (2) a structure in which the sulfonated alkyl chain is directed toward one of the vinyl spacers of the conjugated backbone (Fig. 3b), which will be designated "folded structure" [13]. The folded structure is found to be more stable, [13] due to the decreased distance between the charge sites and the resulting stabilizing non-bonded intramolecular interactions of the sulfoalkyl sidechain with the conjugated backbone. For oligomers 1, in which the sulfoalkyl sidechain is connected to the central ring, and 7, in which the sulfoalkyl sidechain is connected to the peripheral ring, these interactions have been represented in Fig. 4a, b, respectively. In the folded structure of oligomer 1, four intramolecular CH $\cdots$ O interactions involving the oxygen atoms of the SO_3 group stabilize the folded sulfoalkyl sidechain. These interactions are also found for oligomers 2, 3, 4, and 5. Likewise, when the sulfoalkyl sidechain is positioned on a peripheral ring, two of the oxygen atoms of the SO_3 group are involved in four similar CH $\cdots$ O interactions; this is seen for oligomers 7, 8, 9, and 10. The energy differences ΔE between the extended and folded structure ($E_{\text{extended}} - E_{\text{folded}}$) given in Table 1 (disregarding the value of oligomer 5, see below) indicates that stabilization of the folded structure is greater when the sidechain is connected to the peripheral ring.

Oligomers 5 and 6 represent two exceptions. Due to the presence of the two nitrogen atoms next to the central ring, this ring is twisted out of the plane of the peripheral rings and the CH=N spacers by about 40° [14, 15]. Consequently, the SO_3 group of the sidechain is able to contact two of the *ortho*-methoxy groups on the peripheral rings and forms the stabilized structure presented in Fig. 5a, which means that the extended structure that is found for the nine other oligomers (Fig. 3a) does not exist for oligomer 5. A second, more stable folded structure, similar to the ones found for the other nine oligomers (Fig. 3b), was found by replacing the relevant CH functionalities in oligomer 1 (B2 and D1) by nitrogen atoms and reoptimizing the structure. (For numbering of the atoms, see Fig. 6) This explains the small value of 13.88 kJ mol^{-1} for the energy difference for oligomer 5 in Table 1.

The situation for oligomer 6 is reversed. It presents a regular extended structure in which the peripheral rings are twisted out of the molecular plane due to the presence of the nitrogen atoms by about 40°. However, when the folded structure is generated and optimized, one of the CH=N bonds changes its configuration resulting in weak intramolecular CH $\cdots$ O interactions between the SO_3 group and the methoxy groups in the 4- and 6-positions of the peripheral ring (Fig. 5b). Consequently, the SO_3 group is positioned above one of the peripheral rings; even though the negatively charged SO_3 group is in close proximity to the electron-rich peripheral ring, this folded structure is stabilized to a greater extent than the one of oligomer 1 (Table 1).

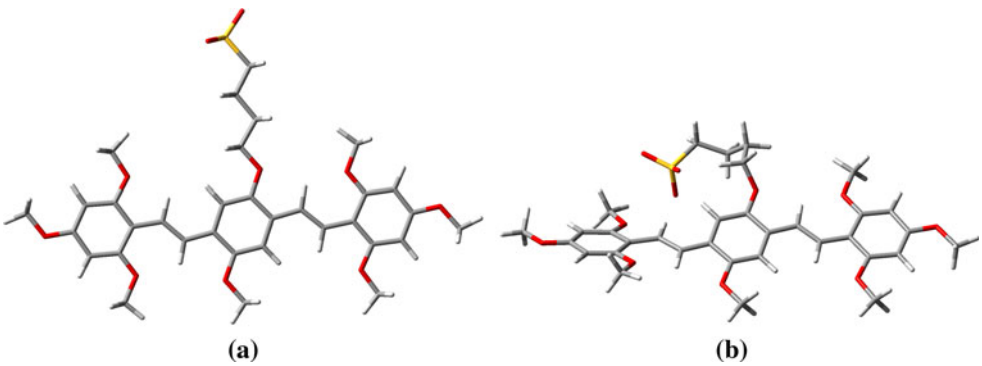

Fig. 3 Different structures of the radical form of the oligomer. **a** Extended structure of the oligomer. **b** Folded structure of the oligomer

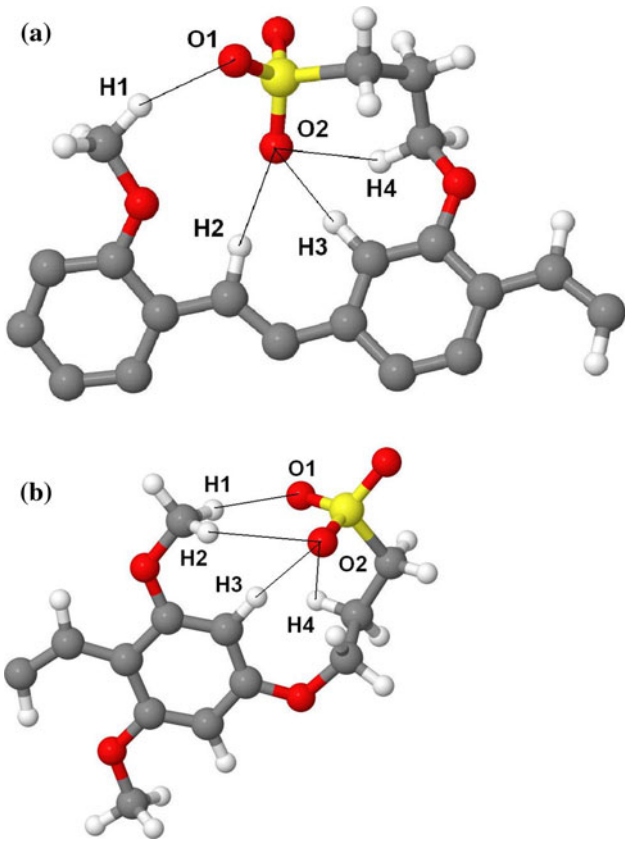

Fig. 4 Intramolecular interactions involving the oxygen atoms of the SO_3 group when the sulfoalkyl sidechain is bonded on the central benzene ring (**a**) or on the outer benzene ring (**b**)

Analysis of the atomic charges using the FOHI method indicates that, regardless of the whereabouts of the SO_3 group and the three-dimensional organization of the folded structure, the SO_3 group always carries a charge of approximately -1. The positive charge is distributed over the entire conjugated backbone, but when nitrogen atoms are present, they carry a significant negative charge and this is linked to a higher spin density.

Table 1 Energy difference ΔE (in $kJ \cdot mol^{-1}$) between the extended and folded radical structures of the ten oligomers

Oligomer	ΔE
1	49.46
2	48.73
3	39.58
4	38.56
5	13.88
6	59.40
7	62.89
8	54.75
9	59.91
10	48.90

$(E_{extended} - E_{folded})$

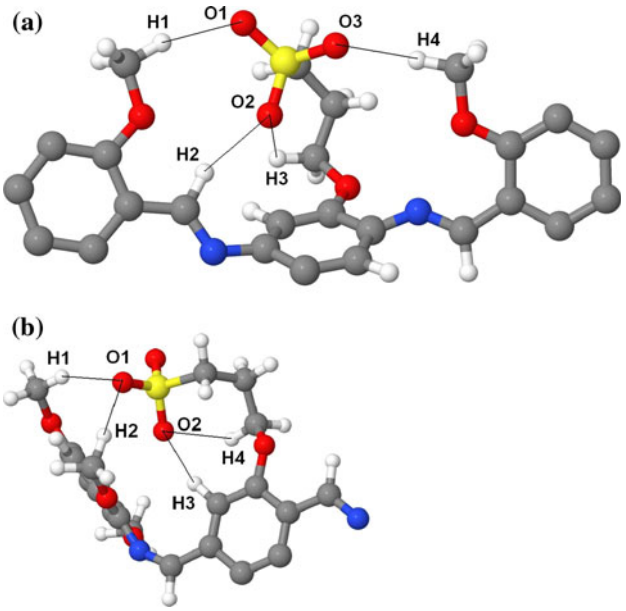

Fig. 5 Intramolecular interactions of the sulfoalkyl sidechain with the conjugated backbone for (**a**) the extended structure of oligomer 5 and (**b**) the folded structure of oligomer 6

4.2 Spin distribution and hyperfine coupling

Based on the FOHI method, atomic spin populations of the ten oligomers were analyzed and compared with the calculated EPR parameters. Because of the large number of atoms for the different oligomers, the changes in the atomic spin populations of the radicals are represented by dividing each oligomer into six fragments. As presented in Fig. 6, these comprise each of the two peripheral rings with substituents (A and E), the central ring (C), the two vinyl spacers (B and D), and the sidechain (S). The results can be found in Table 2. The maximum ^{1}H and ^{14}N hyperfine couplings and the positions of the relevant atoms in the structure can be found in Table 3.

The maximum ^{1}H hyperfine coupling of oligomer 1 has been determined experimentally [16] and has a value of about 10.9 MHz. The absolute value of the calculated hyperfine coupling for hydrogen (D2) is about 11.6 MHz, in good agreement with the experimental value. The absence of the methoxy group on the central benzene ring $(1 \rightarrow 2)$ does not seem to have a significant influence. The spin populations in Table 2 suggest that there is only a slight reorganization of the spin and then mostly on the central ring, which is also seen in the results of the EPR calculations. Upon introducing one nitrogen atom into the sulfoalkyl sidechain $(1 \rightarrow 3)$, a considerable amount of spin becomes located on the sidechain (Table 2) and then mostly on the nitrogen atom. Therefore, for oligomer 3, the proton *alpha* to the nitrogen atom in the sidechain has the

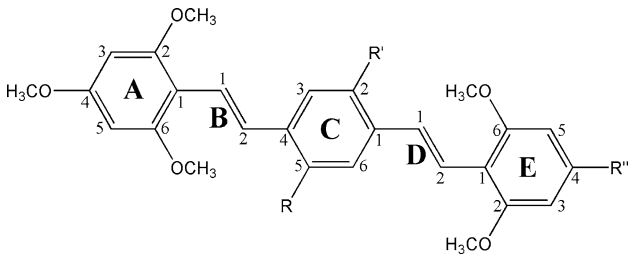

Fig. 6 Labeling of the atoms in the conjugated backbone and schematic representation of the different groups in which the atomic spin has been summed. R' and R'' indicate the sulfoalkyl sidechain or a methoxy group. R is a methoxy group or a hydrogen atom

highest ^{1}H hyperfine coupling. Removing the methoxy group from the central benzene ring $(3 \rightarrow 4)$ again changes the spin distribution significantly in the central ring (C), but also in the sidechain (S). The difference with respect to the ^{14}N hyperfine coupling is considerable, and this can be explained by the absence of the mesomeric interaction between the methoxy group and the aniline moiety in oligomer 4.

For oligomer 5, the spin is mainly localized on the central ring (C) and the vinyl spacer B, and the maximum ^{1}H hyperfine coupling is found for the hydrogen atom in the CH=N group, which interacts with the sulfoalkyl sidechain. This is reflected in the increased values of both the ^{1}H and ^{14}N hyperfine coupling. As expected, for oligomer 6, the spin shifts almost completely to peripheral benzene ring A and vinyl spacer B, which interact with the sulfoalkyl sidechain. This considerable spin localization is clearly reflected in the large values of the ^{1}H and ^{14}N hyperfine coupling constants.

As expected for oligomer 7, moving the sulfoalkyl sidechain to peripheral ring E leads to a shift of the spin distribution in the conjugated backbone to this ring; the presence or absence of methoxy groups on the central ring (oligomer 9) does not change, and therefore, the ^{1}H hyperfine coupling constants are similar. Introduction of a single nitrogen atom in the conjugated backbone $(7 \rightarrow 8)$ leads to an increase in the spin delocalization, and again the largest ^{1}H hyperfine coupling is found for the hydrogen atom in the CH=N spacer. Introduction of two nitrogen atoms $(7 \rightarrow 10)$ leads to a higher spin density in fragments C, D, and E, which results in a higher ^{1}H hyperfine coupling in oligomer 10 than in oligomer 8.

Table 2 Spin population of the different groups in the oligomers as defined in Fig. 6

Oligomer	A	B	C	D	E	S
1	0.22	0.20	0.34	0.11	0.11	0.02
2	0.23	0.20	0.28	0.14	0.13	0.01
3	0.14	0.12	0.45	0.08	0.09	0.13
4	0.18	0.16	0.35	0.12	0.12	0.08
5	0.08	0.18	0.52	0.12	0.03	0.06
6	0.65	0.31	0.03	0.00	0.00	0.01
7	0.09	0.08	0.24	0.21	0.33	0.05
8	0.14	0.14	0.28	0.16	0.23	0.04
9	0.09	0.08	0.18	0.22	0.36	0.06
10	0.05	0.11	0.32	0.20	0.27	0.05

Table 3 Absolute values of the maximum ^{1}H and ^{14}N hyperfine coupling constants (in MHz) of the ten oligomers and the position in the structure

Oligomer	^{1}H Hyperfine coupling	Position	^{14}N Hyperfine coupling	Position
1	11.6	D2		
2	12.2	D2		
3	14.1	Sidechain	6.3	Sidechain
4	13.3	D2	3.6	Sidechain
5	28.2	B1	20.7	B2
6	51.3	B2	39.9	B1
7	12.8	D1		
8	19.9	D2	12.8	D1
9	15.3	D1		
10	25.5	D2	15.7	D1

5 Conclusion

A set of self-doping PPV oligomers has been studied using quantum chemical calculations in order to analyze the effects of different functionalities on the geometry of the self-doped structure, its spin distribution obtained using the FOHI method, and the resulting maximum hyperfine coupling constants. Moving the sidechain from the central ring to the peripheral ring does not significantly change the spin distribution nor the values of the EPR parameters, but it does lead to an increased stability of the self-doped system. Of all the studied structures, oligomer 8 is the best candidate to replace oligomer 1, as it combines a similar spin distribution with an increased ^{1}H hyperfine coupling, an additional ^{14}N hyperfine coupling and a CH=N spacer, which allows the preparation and full purification of an OH-substituted oligomer.

Acknowledgments This work was carried out using the Turing HPC infrastructure at the CalcUA core facility of the University of Antwerp, a division of the Flemish Supercomputer Center VSC, funded by the Hercules Foundation, the Flemish Government (department EWI) and the Universiteit Antwerpen. Financial support by the University of Antwerp under Grant GOA-2404 is gratefully

acknowledged. AK is greatful to the Research Foundation—Flanders (FWO) for a postdoctoral position and financial support.

References

1. Tachelet W, Jacobs S, Ndayikengurukiye H, Geise HJ, Grner J (1994) Appl Phys Lett 64:2364–2366
2. Yang JP, Heremans PL, Hoefnagels R, Tachelet W, Dieltiens P, Blockhuys F, Geise HJ, Borghs G (2000) Synth Met 108:95–100
3. Yang JP, Jin YD, Heremans PL, Hoefnagels R, Dieltiens P, Blockhuys F, Geise HJ, Vander Auweraer M, Borghs G (2000) Chem Phys Lett 325:251–256
4. Jin YD, Chen HZ, Heremans PL, Aleksandrzak K, Geise HJ, Borghs G, Vander Auweraer M (2002) Synth Met 127:155–158
5. Chen HZ, Jin YD, Xu RS, Peng BX, Desseyn H, Janssens J, Heremans P, Borghs G, Geise HJ (2003) Synth Met 139:529–534
6. Ding XB, Zheng JG, Jin YD, Heremans PL, Geise HJ, Borghs G (2003) Synth Met 137:1003–1004
7. Ding XB, Zheng JG, Jin YD, Aerts G, Peng BX, Heremans PL, Borghs G, Geise HJ (2004) Synth Met 142:267–273
8. Staes E, Nagels LJ, Verreyt G, Jacobs S, Bao Y, Geise HJ (1997) Electroanalysis 9:1197–1200
9. Poels I, Nagels LJ, Verreyt G, Geise HJ (1998) Anal Chim Acta 370:105–113
10. Szymaska I, Ocicka K, Radecka H, Radecki J, Geise HJ, Dieltiens P, Aleksandrzak K (2001) Mat Sci Eng C 18:171–176
11. Zimkus A, Cretscu I, Grzybowska I, Radecka H, Geise HJ, Dieltiens P, Aleksandrzak K (2003) Pol J Environ Stud 12:773–778
12. Collas A, De Borger R, Amanova T, Vande Velde CML, Baeke JK, Dommisse R, Van Alsenoy C, Blockhuys F (2011) New J Chem 35:649–662
13. Baeke JK, De Borger R, Lemire F, Van Alsenoy C, Blockhuys F (2009) J Phys Org Chem 22:925–932
14. Collas A, De Borger R, Amanova T, Blockhuys F (2011) CrystEngComm 13:702–710
15. Collas A, Zeller M, Blockhuys F (2011) Acta Cryst C 67:o171–o174
16. Ling Y, Kozakiewicz P, Blockhuys F, Biesemans M, Van Alsenoy C, Moons H, Goovaerts E, Willem R, Van Doorslaer S (2011) Phys Chem Chem Phys 13:18516–18522
17. Hirshfeld FL (1977) Theoret Chem Acta 44:129–138
18. Bultinck P, Van Alsenoy C, Ayers PW, Carbo-Dorca R (2007) J Chem Phys 126:144111
19. Bultinck P, Ayers PW, Fias S, Tiels K, Van Alsenoy C (2007) Chem Phys Lett 444:205
20. Geldof D, Krishtal A, Blockhuys F, Van Alsenoy C (2011) J Chem Theory Comput 7:1328–1335
21. Becke AD (1993) J Chem Phys 98:5648–5652
22. Lee C, Yang W, Parr RG (1988) Phys Rev B 37:785–789
23. Vosko SH, Wilk L, Nusair M (1980) Can J Phys 58:1200–1211
24. Stephens PJ, Devlin FJ, Chabalowski CF, Frisch MJ (1994) J Phys Chem 98:11623–11627
25. Krishnan R, Binkley JS, Seeger R, Pople JA (1980) J Chem Phys 72:650–654
26. Gaussian 09, Revision A.02, Frisch MJ, Trucks GW, Schlegel HB, Scuseria GE, Robb MA, Cheeseman JR, Scalmani G, Barone V, Mennucci B, Petersson GA et al (2009) Gaussian, Inc., Wallingford CT
27. Neese F (2008) ORCA an ab initio, density functional and semiempirical program package, Version 2.6. University of Bonn, Bonn
28. Barone V (1996) Recent advances in density functional methods. World Scientific Publ. Co., Singapore
29. Schaefer A, Horn H, Ahlrichs RJ (1992) Chem Phys 97:2571–2577
30. The Ahlrichs (2df,2pd) polarization functions were obtained from the TurboMole basis set library under ftp.chemie.uni-karlsruhe.de/pub/basen, R. Ahlrichs and co-workers (unpublished)
31. Van Alsenoy C, Peeters A (1993) J Mol Struct (Theochem) 286:19
32. Rousseau B, Peeters A, Van Alsenoy C (2000) Chem Phys Lett 324:189